

# Experimental study of the polyamorphism of water. II. The isobaric transitions between HDA and VHDA at intermediate and high pressures

Philip H. Handle, and Thomas Loerting

Citation: *The Journal of Chemical Physics* **148**, 124509 (2018); doi: 10.1063/1.5019414

View online: <https://doi.org/10.1063/1.5019414>

View Table of Contents: <http://aip.scitation.org/toc/jcp/148/12>

Published by the [American Institute of Physics](#)

---

## Articles you may be interested in

[Experimental study of the polyamorphism of water. I. The isobaric transitions from amorphous ices to LDA at 4 MPa](#)

*The Journal of Chemical Physics* **148**, 124508 (2018); 10.1063/1.5019413

[Equilibration and analysis of first-principles molecular dynamics simulations of water](#)

*The Journal of Chemical Physics* **148**, 124501 (2018); 10.1063/1.5018116

[Comment on "The putative liquid-liquid transition is a liquid-solid transition in atomistic models of water" \[I and II: \*J. Chem. Phys.\* 135, 134503 \(2011\); \*J. Chem. Phys.\* 138, 214504 \(2013\)\]](#)

*The Journal of Chemical Physics* **148**, 137101 (2018); 10.1063/1.5029463

[Microscopic structural descriptor of liquid water](#)

*The Journal of Chemical Physics* **148**, 124503 (2018); 10.1063/1.5024565

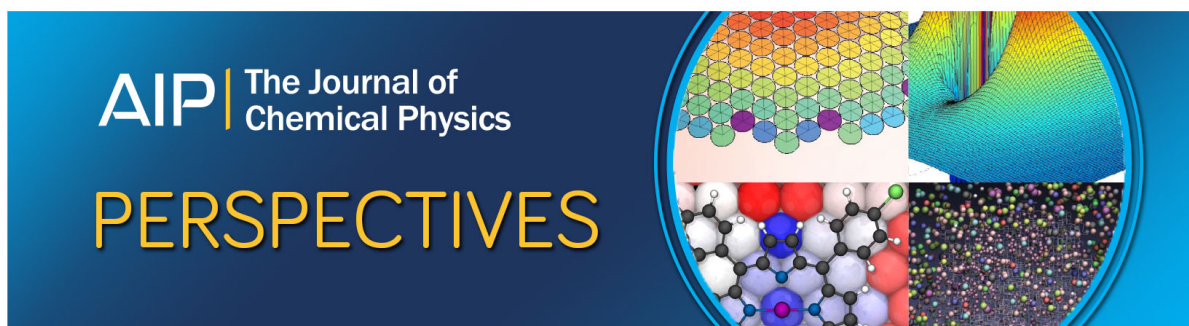
[Potential energy landscape of TIP4P/2005 water](#)

*The Journal of Chemical Physics* **148**, 134505 (2018); 10.1063/1.5023894

[The barrier to ice nucleation in monatomic water](#)

*The Journal of Chemical Physics* **148**, 124505 (2018); 10.1063/1.5016518

---



# Experimental study of the polyamorphism of water. II. The isobaric transitions between HDA and VHDA at intermediate and high pressures

Philip H. Handle<sup>a)</sup> and Thomas Loerting<sup>b)</sup>

*Institute of Physical Chemistry, University of Innsbruck, Innrain 52c, A-6020 Innsbruck, Austria*

(Received 14 December 2017; accepted 27 February 2018; published online 30 March 2018)

Since the first report of very-high density amorphous ice (VHDA) in 2001 [T. Loerting *et al.*, Phys. Chem. Chem. Phys. **3**, 5355–5357 (2001)], the status of VHDA as a distinct amorphous ice has been debated. We here study VHDA and its relation to expanded high density amorphous ice (eHDA) on the basis of isobaric heating experiments. VHDA was heated at  $0.1 \leq p \leq 0.7$  GPa, and eHDA was heated at  $1.1 \leq p \leq 1.6$  GPa to achieve interconversion. The behavior upon heating is monitored using *in situ* volumetry as well as *ex situ* X-ray diffraction and differential scanning calorimetry. We do not observe a sharp transition for any of the isobaric experiments. Instead, a continuous expansion (VHDA) or densification (eHDA) marks the interconversion. This suggests that a continuum of states exists between VHDA and HDA, at least in the temperature range studied here. This further suggests that VHDA is the most relaxed amorphous ice at high pressures and eHDA is the most relaxed amorphous ice at intermediate pressures. It remains unclear whether or not HDA and VHDA experience a sharp transition upon isothermal compression/decompression at low temperature. © 2018 Author(s). All article content, except where otherwise noted, is licensed under a Creative Commons Attribution (CC BY) license (<http://creativecommons.org/licenses/by/4.0/>). <https://doi.org/10.1063/1.5019414>

## I. INTRODUCTION

Water, the molecule of life, is ubiquitous in nature and yet bears astonishing properties. Those properties, often called anomalies, are nicely listed on the web page of Martin Chaplin.<sup>1</sup> An attempt to explain some of those anomalies invokes the existence of a second critical point in the phase diagram of water, marking the end-point of a hypothetical binodal that separates two liquid phases.<sup>2–5</sup> It is further suspected that those two liquids have amorphous counterparts, namely, high-density amorphous ice (HDA) and low-density amorphous ice (LDA),<sup>6,7</sup> both of which were first reported by Mishima *et al.*<sup>8,9</sup> Hence, the existence of distinct amorphous forms, a phenomenon called polyamorphism, hints at the existence of distinct liquids. Since the third amorphous ice form called very high-density amorphous ice (VHDA) was reported in 2001,<sup>10</sup> naturally the question arose whether water could even form three distinct liquids. Although being highlighted about a decade ago,<sup>3,11</sup> the status of VHDA is still an open question.

In attempting to answer this question, one has to clarify whether VHDA is a truly distinct polyamorph or not. Since we devoted a fair share of the Introduction in Paper I<sup>12</sup> to the general discussion of polyamorphism, we are not going to dwell on this any further here. We simply state that if VHDA is a distinct polyamorph it has to share a first-order-like transition

with other amorphous ices. Given that studies of VHDA both during isobaric heating at low pressures<sup>12–16</sup> and isothermal decompression at  $T \geq 125$  K<sup>17,18</sup> showed that VHDA transforms to HDA before it transforms to LDA, the key question on the status of VHDA boils down to the clarification of the HDA-VHDA relation.

### A. The relation of HDA and VHDA

VHDA is usually produced by heating HDA at pressures exceeding 0.8 GPa.<sup>10</sup> HDA itself is produced by pressure induced amorphisation (PIA), i.e., compressing hexagonal ice at 77 K to pressures above 1.0 GPa.<sup>8</sup> This HDA obtained from PIA is commonly referred to as unannealed HDA (uHDA).<sup>19</sup> It is contrasted with relaxed HDA forms exhibiting lower density than uHDA, called expanded HDA (eHDA). Routes to eHDA are isobaric heating of uHDA at pressures below 0.5 GPa<sup>19,20</sup> or decompression of VHDA at 140 K to pressures below 0.4 GPa.<sup>17</sup> Based on its high thermal stability at ambient pressure,<sup>19–21</sup> eHDA is regarded as a highly relaxed form of HDA.

The preparation of VHDA involves a transformation from uHDA.<sup>10</sup> This transformation involves a sudden, but small change in density, and hence it is hard to characterize the nature of the transition. A kink in the density versus pressure curve was reported around 0.8 GPa indicating a possible, albeit very small discontinuity.<sup>22</sup> Even if there is no, or only a very small, discontinuity in density, there is a clear difference in  $\partial\rho/\partial p$ , which for VHDA is smaller ( $0.10 \text{ g cm}^{-3} \text{ GPa}^{-1}$ ) than for HDA ( $0.21 \text{ g cm}^{-3} \text{ GPa}^{-1}$ ).<sup>22</sup> Further evidence for a jump-like transformation from HDA to VHDA was provided by *ex situ* Raman-spectroscopy,<sup>22</sup> a possible

<sup>a)</sup>Present address: Department of Physics, Sapienza University of Rome, Piazzale Aldo Moro 5, I-00185 Roma, Italy.

<sup>b)</sup>Author to whom correspondence should be addressed: thomas.loerting@uibk.ac.at

maximum in the relaxation dynamics<sup>23</sup> and corresponding glass-to-liquid transition temperatures.<sup>23,24</sup> Most prominently two density jumps were found during isothermal compression of LDA at 125 K.<sup>25</sup> The first jump at 0.45 GPa corresponds to the LDA  $\rightarrow$  HDA transition and the second one at 0.95 GPa was assigned to the HDA  $\rightarrow$  VHDA transition.<sup>25</sup> Based on ambient pressure structures, it was argued<sup>11</sup> that those two transitions should be similar since the coordination number (defined to 3.3 Å) changes from four (LDA) to five (HDA) to six (VHDA).<sup>26,27</sup>

On the other hand, there are a number of studies, in which a jump-like transformation from HDA to VHDA could not be identified. Mishima<sup>28</sup> used similar high-pressure annealing as Loerting *et al.*,<sup>10</sup> but stated that all states found were variations of a single polymorph, i.e., HDA. This is supported by a more recent study reporting no kink in the density versus pressure curve at  $\approx$ 0.8 GPa, implying also a smooth change in compressibility.<sup>29</sup> In addition, the HDA  $\rightarrow$  VHDA density step reported at 125 K<sup>25</sup> was not found in a volumetric study by Mishima<sup>30</sup> utilizing a similar path but much higher compression rates, or upon compression of LDA at 100 K.<sup>25</sup> Furthermore, an *in situ* Raman spectroscopy study of the isothermal compression of LDA at 135 K by Yoshimura *et al.* does not report a HDA  $\rightarrow$  VHDA transition.<sup>31</sup> Since Loerting *et al.*<sup>25</sup> reported that the lower the compression rate is, the sharper the step is. Mishima's rate of 0.6 GPa min<sup>-1</sup><sup>30</sup> might have been too high to see this step. Yoshimura *et al.*<sup>31</sup> did not report a step presumably since they are lacking measurements in the relevant pressure range and/or since they worked at higher temperature. Still, different results were also obtained for LDA<sub>II</sub>, a relaxed form of LDA (cf. Ref. 32 for details on LDA<sub>II</sub>). When LDA<sub>II</sub> is compressed at 125 K, no second step, corresponding to a HDA  $\rightarrow$  VHDA transition, is found.<sup>33</sup> Moreover, the decompression of VHDA between 125 and  $\approx$ 140 K shows a continuous evolution of VHDA to HDA.<sup>17,18</sup> Similar results were presented for isobaric paths.<sup>12-14,16</sup> Finally, results from high-pressure scattering experiments<sup>34,35</sup> and spectroscopy<sup>29</sup> also point toward VHDA and HDA becoming increasingly similar at increasing pressure.

We note that the status of VHDA is unclear not only in pure, but also in salty water.<sup>36-38</sup> While a first-order-like HDA  $\rightarrow$  VHDA transition was reported in LiCl-H<sub>2</sub>O, it could not be identified in NaCl-H<sub>2</sub>O. Also in numerical studies, the results are ambiguous. Even though multiple liquid-liquid transitions are possible in principle<sup>39</sup> and have also been reported for water models,<sup>40-43</sup> the majority of results report a continuum of states between VHDA and HDA.<sup>44-49</sup> Besides, the results of Refs. 42 and 43 were criticized<sup>50</sup> for their treatment of long-range interactions.

## B. Aim of this work

If one assumes the existence of a binodal separating VHDA and HDA, it should be located around a pressure of 0.8 GPa based on studies favouring a separation. This hypothesis is schematically depicted in Fig. 1(a). As recently suggested by us, this hypothesis involves a low-lying critical point above which the distinction between HDA and VHDA disappears.<sup>23</sup> According to this scheme, HDA should be thermodynamically more stable at lower pressures and VHDA at higher pressures.

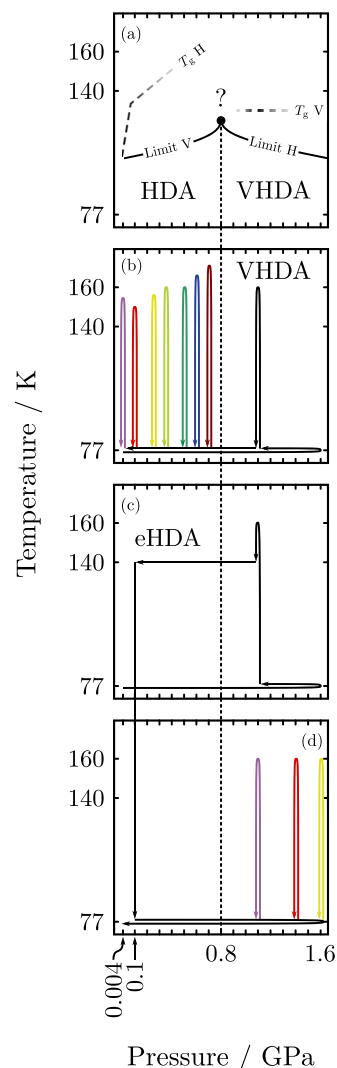


FIG. 1. (a) Schematic phase diagram indicating a possible critical point ending a binodal (dotted line) separating HDA and VHDA. The corresponding limits of stability (solid lines) are also shown. The dashed lines are the approximate location of the glass-to-liquid transition  $T_g$  based on Ref. 24. The other parts show the experimental paths taken to test for the occurrence of stability limits: Part (b) shows the VHDA-path: hexagonal ice is compressed at 77 K and subsequently heated at 1.1 GPa. Upon reaching 160 K, the sample is quenched to 77 K and brought to  $0.1 \leq p \leq 0.7$  GPa. At the final pressure, the sample is heated again and then quench-recovered to 77 K and 1 bar. Parts (c) and (d) show the eHDA path: hexagonal ice is compressed at 77 K and subsequently heated at 1.1 GPa. Upon reaching 160 K, the sample is cooled to 140 K and decompressed. Upon reaching 0.1 GPa, the sample is quenched to 77 K. The sample is then recompressed to  $1.1 \leq p \leq 1.6$  GPa where it is heated again to 160 K and quench-recovered to 77 K and 1 bar.

However, because of kinetic limitations at 77 K, HDA can be compressed to pressures beyond 0.8 GPa without transforming to VHDA<sup>8,10</sup> and VHDA can be recovered to ambient pressure without transforming to HDA.<sup>10,18</sup> Similar kinetic hindrance is observed for the HDA-LDA case, where a large hysteresis is present.<sup>30</sup> Besides the binodal, however, limits of stability have to exist at which the amorphous ices inevitably experience a polyamorphic transition. Again, those limits were charted for the LDA-HDA case and sharp first-order-like transitions were found.<sup>9,12,17,20,21,30,32,51</sup> We here aim to investigate the possible existence of such stability limits for the HDA-VHDA case. To this end, we study both the behavior

of VHDA during isobaric heating at  $0.1 \leq p \leq 0.7$  GPa (i.e., in the metastability domain of HDA) to look for signs of a VHDA  $\rightarrow$  eHDA transition and the isobaric heating behavior of eHDA at  $1.1 \leq p \leq 1.6$  GPa (i.e., in the metastability domain of VHDA) to look for signs of an eHDA  $\rightarrow$  VHDA transition. The isobaric heating steps are monitored by *in situ* volumetry and the samples are further characterized *ex situ* using powder X-ray diffraction (XRD) and differential scanning calorimetry (DSC).

## II. EXPERIMENTAL DETAILS

In order to produce the different samples, 500  $\mu\text{l}$  of pure water was pipetted into a preformed indium container ( $m \approx 320$  mg) at 77 K. Indium serves as a low-temperature lubricant, a technique pioneered by Mishima *et al.*<sup>8</sup> The samples were then put in a high-pressure cell of 8 mm bore diameter, and the cell was subsequently placed in a material testing machine (Zwick model BZ100/TL3S; for details on our apparatus, see Ref. 52). The pressure was raised to 1.0 GPa at 77 K to push the air out of the sample, reduced to 0.02 GPa and subsequently raised again to 1.5–1.7 GPa with  $0.14$  GPa  $\text{min}^{-1}$ . During the last step, the ice sample transforms to uHDA via PIA. The pressure was subsequently reduced to 1.1 GPa. Then the samples were heated isobarically with  $3$  K  $\text{min}^{-1}$  to 160 K to produce VHDA. After reaching 160 K, two different paths were taken: the VHDA-path [cf. Fig. 1(b)] and the eHDA-path [cf. Figs. 1(c)–1(d)].

For the VHDA-path, the samples were quenched with liquid  $\text{N}_2$  after reaching 160 K and decompressed at 77 K to  $0.1 \leq p \leq 0.7$  GPa with a rate of  $0.14$  GPa  $\text{min}^{-1}$ . After reaching the desired pressure, the VHDA samples were heated with  $3$  K  $\text{min}^{-1}$  to temperatures between 98 and 167 K and quenched with liquid  $\text{N}_2$  thereafter. This step serves the purpose of investigating the VHDA  $\rightarrow$  eHDA transformation. After the quench procedure, the samples were brought back to ambient pressure with a rate of  $0.14$  GPa  $\text{min}^{-1}$ , pushed out of the pressure cell, stored at 77 K, and characterized by x-ray diffraction (XRD) and differential scanning calorimetry (DSC). Additionally one VHDA sample was completely decompressed at 77 K without heating at lower pressure. This sample serves as the VHDA reference here.

For the eHDA-path, the samples were cooled at 1.1 GPa to 140 K. Then the samples were isothermally decompressed to 0.1 GPa with  $0.02$  GPa  $\text{min}^{-1}$  and quenched with liquid  $\text{N}_2$  upon reaching 0.1 GPa. This results in eHDA.<sup>17</sup> The samples were then recompressed to pressures between 1.1 and 1.6 GPa at 77 K, where eHDA was heated isobarically with  $3$  K  $\text{min}^{-1}$  to 160 K. This step serves the purpose of investigating the eHDA  $\rightarrow$  VHDA transformation. After reaching 160 K, the samples were quenched and recovered and characterized as explained for the VHDA path. Additionally, one eHDA sample was completely decompressed after quench at 0.1 GPa without recompression and heating at high pressure. This sample serves as the eHDA reference here.

During all high-pressure steps, *in situ* dilatometry was performed by recording the piston displacement. The piston displacement curves were converted to change of volume

curves assuming constant cell diameter and correcting for the apparatus behavior by subtracting a blind experiment. For the blind experiment, we perform the same steps as for the real experiment, leaving only the water out. Thus, we are able to record the behavior of the apparatus and the indium along the studied paths (cf. Ref. 53).

For the purpose of recording X-ray diffractograms, the samples were first divided into two or three pieces and each piece was powdered and measured separately. Hence, two or three diffractograms were recorded per sample. Division and powdering were performed in liquid  $\text{N}_2$ . The powder was cold-loaded onto a precooled ( $\approx 80$  K) nickel-plated copper sample holder in flat geometry. The low-temperature chamber by Anton-Paar (TTK 450) holding the sample holder is then closed and pumped to approximately  $10^{-2}$  mbar. We used a Siemens D 5000 diffractometer equipped with a Cu-K $\alpha$  x-ray source ( $\lambda = 1.541$  Å) to record the diffractograms at  $\approx 80$  K from  $2\theta = 10^\circ$  ( $K = 0.71$  Å $^{-1}$ ) to  $2\theta = 54^\circ$  ( $K = 3.70$  Å $^{-1}$ ) using a step width of  $0.02^\circ$  and acquisition time of 1 s per step. The phase composition of crystalline samples containing more than one polymorph was determined using PowderCell (version 2.4, BAM, Bundesanstalt für Materialforschung und -prüfung, Berlin, Germany). The relevant structural data were taken from Refs. 54–63 for several ice polymorphs and from Ref. 64 for our nickel-plated copper sample holder.

For the purpose of recording DSC heating scans, small parts of the sample were put in DSC-crucibles at 77 K. The crucibles were placed into the 93 K pre-thermostated DSC-instrument (Perkin-Elmer DSC 8000). Thermograms were recorded in two subsequent scans with a heating rate of  $10$  K  $\text{min}^{-1}$ : A first scan from 93 to 233 K to record the latent heat of the irreversible transformation(s) and a second scan from 93 to 293 K. The second scan serves as baseline for the first scan and is used to calculate the sample mass from the melting endotherm of hexagonal ice.

## III. ISOBARIC HEATING OF VHDA

### A. Analysis of the volume curves

The volume curves of the isobaric heating experiments with VHDA samples at different pressures in the metastability domain of HDA are shown in Fig. 2(a). The starting points of the curves include the volume change during decompression, i.e., the curves show  $V_m(T) - V_m^{\text{VHDA}}(77 \text{ K}, 1.1 \text{ GPa})$ . For example, for the 0.1 GPa curve in Fig. 2(a), the starting point at  $0.8 \text{ cm}^3 \text{ mol}^{-1}$  implies that VHDA expands by  $0.8 \text{ cm}^3 \text{ mol}^{-1}$  upon decompression from 1.1 GPa to 0.1 GPa.

All curves show that heating results in an expansion of the VHDA samples. The expansion always consists of two stages: (i) a non-linear stage at low temperatures and (ii) a sharp step at higher temperatures marking the crystallization of the sample. The shape of the volume curves suggests that the samples relax in a continuous fashion toward higher molar volume before this relaxation is terminated by crystallization.

It is further evident that the lower the pressure is, the more non-linear expansion is seen. This is not surprising since VHDA is a relaxed amorphous ice at 1.1 GPa, but not at other pressures. Lowering the pressure and heating the sample

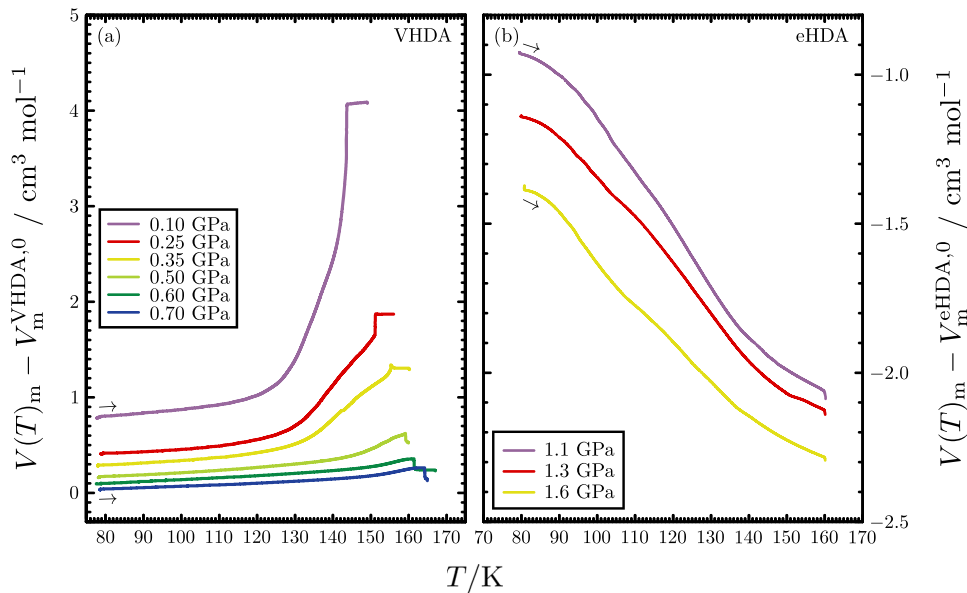


FIG. 2. *In situ* volumetry of the isobaric heating of VHDA (a) and eHDA (b) at different pressures.  $V_m^{\text{VHDA},0} = V_m^{\text{VHDA}}(77 \text{ K}, 1.1 \text{ GPa})$  and  $V_m^{\text{eHDA},0} = V_m^{\text{eHDA}}(77 \text{ K}, 0.1 \text{ GPa})$ .

yield relaxation toward lower density, i.e., expansion. The further the deviation from 1.1 GPa, the more expansion is expected.

This line of reasoning explains also a difference to uHDA. While the VHDA samples expand at all pressures studied here, uHDA is known to expand during isobaric heating below 0.35 GPa,<sup>29,65</sup> but it compacts at higher pressures.<sup>29</sup> In other words, the initial density of uHDA at  $p < 0.35$  GPa is lower than the density in the relaxed state, whereas the initial density of VHDA is always higher than the density in the relaxed state at all pressures  $\leq 0.7$  GPa.

## B. XRD and DSC analysis

To characterize the states that appear when VHDA is heated isobarically, the experiments corresponding to the lines in Fig. 2(a) were repeated several times and quenched at different temperatures. Those quenched samples were recovered to ambient pressure at 77 K and characterized by XRD and DSC. The quench temperatures are indicated in Figs. 3–5 by coloured symbols on the volume curves (left panels), which are reproduced from Fig. 2(a). Figures 3–5 cover the pressure ranges 0.10–0.25 GPa, 0.35–0.50 GPa, and 0.60–0.70 GPa,

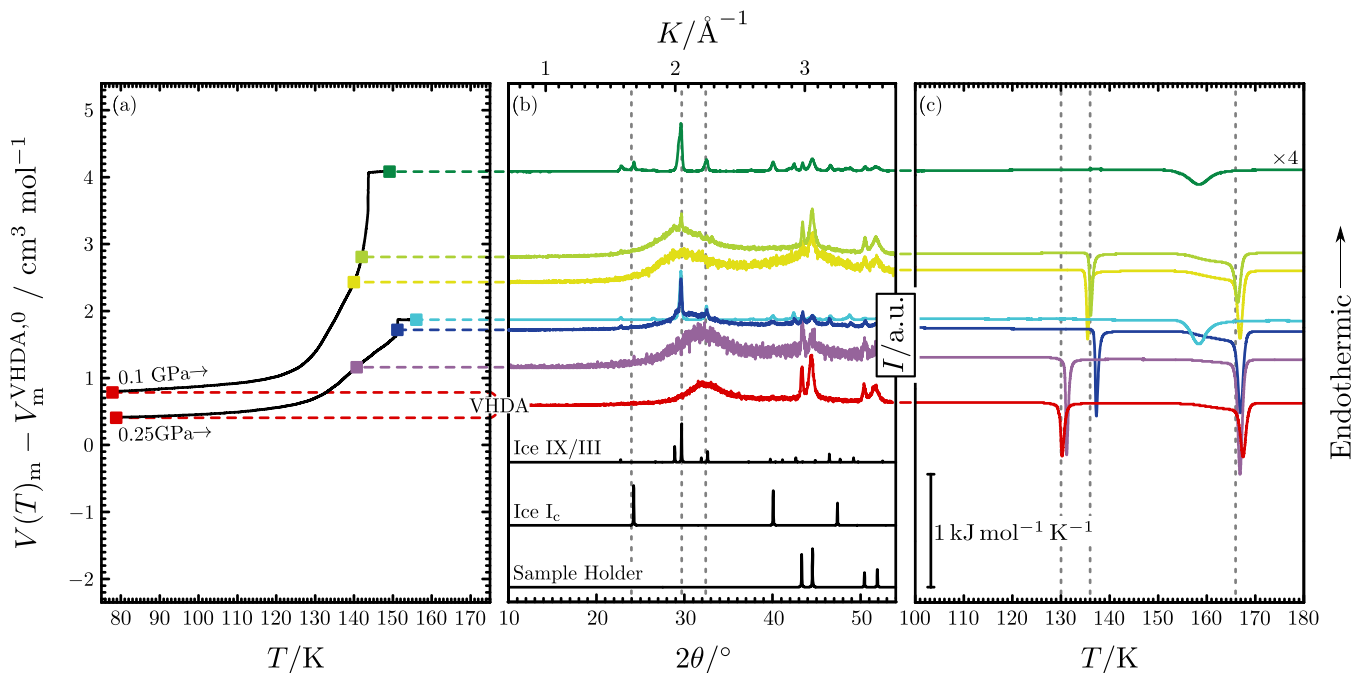


FIG. 3. XRD and DSC analysis of intermediate states of the isobaric heating of VHDA at 0.1 and 0.25 GPa. (a) shows the volume change and the squares mark temperatures of quench-recovery. The corresponding diffractograms and calorigrams after quench-recovery are shown in (b) and (c), respectively. In (b), the dotted grey line at  $24.0^\circ$  ( $1.69 \text{ \AA}^{-1}$ ) marks the position of the first diffraction maximum for LDA according to Refs. 80 and 32. The dotted grey lines at  $29.7^\circ$  ( $2.09 \text{ \AA}^{-1}$ ) and at  $32.4^\circ$  ( $2.26 \text{ \AA}^{-1}$ ) mark the position of the first diffraction maximum of the eHDA and VHDA references, respectively. The black diffractograms at the bottom of (b) are calculated diffractograms of ice  $I_c$ , ice IX/III and the sample holder. In (c), the dotted grey lines at 130, 136, and 166 K mark the onset temperature of the VHDA  $\rightarrow$  LDA, eHDA  $\rightarrow$  LDA, and LDA  $\rightarrow$   $I_c$  transition, respectively.

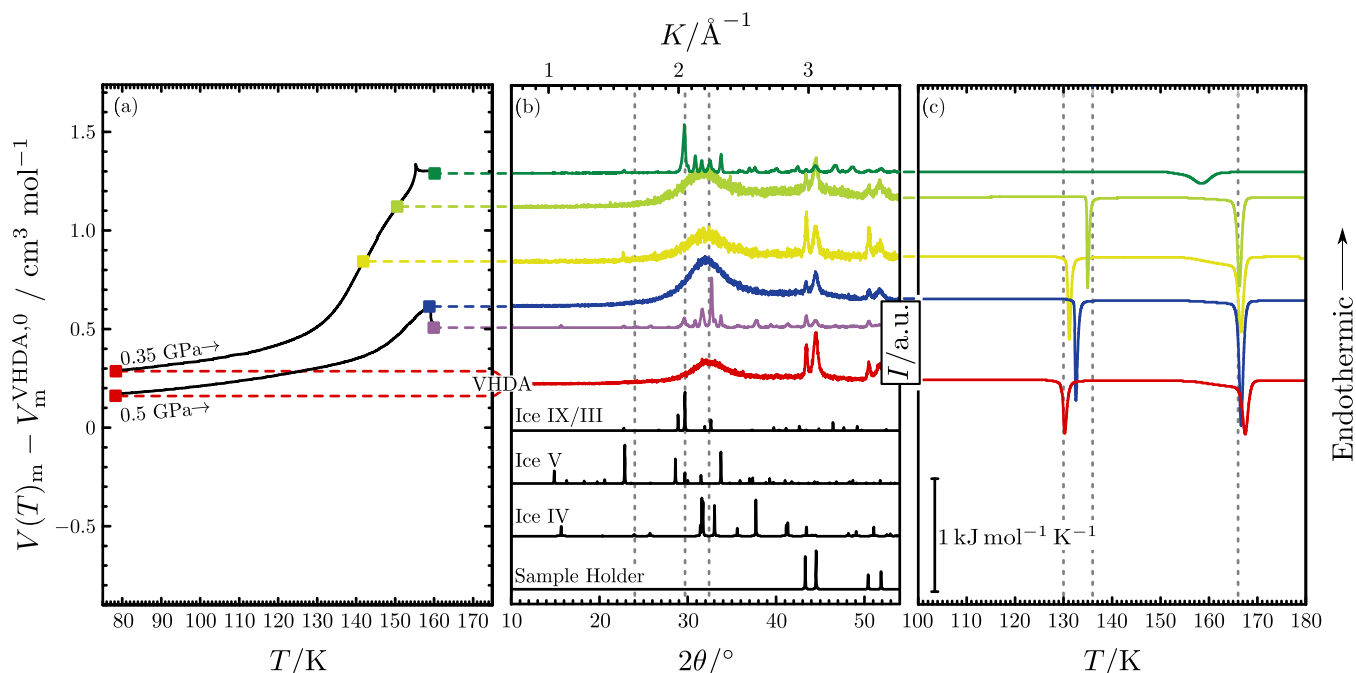


FIG. 4. Analogous to Fig. 3 for heating of VHDA at 0.35 and 0.50 GPa. The black diffractograms at the bottom of (b) are calculated diffractograms of ice IX/III, ice V, ice IV and the sample holder.

respectively. In addition, XRD scans (middle panel) and DSC scans (right panel) are shown, where each scan has the same colour code as the symbols and is connected by the horizontal dashed line with the symbols.

From X-ray diffractograms, amorphous samples are easily distinguished from crystalline samples since they lack sharp reflexes and only show broad halo peaks. Our criterion for the state of relaxation in amorphous samples is the location of the maximum of the first halo peak ( $2\theta_{\max}$ ).

In DSC scans, high density amorphous ice (VHDA or HDA) shows two exotherms:<sup>20,21,28,66,67</sup> (i) the amorphous-amorphous transition to LDA and (ii) the crystallization of LDA to cubic ice. By contrast, high-pressure crystalline ices show only one exotherm,<sup>68–72</sup> namely, the polymorphic transition to stacking-disordered cubic ice.<sup>73,74</sup> Our criterion for the state of relaxation in amorphous samples is the onset temperature of the first exotherm, which we denote  $T_e$  here.

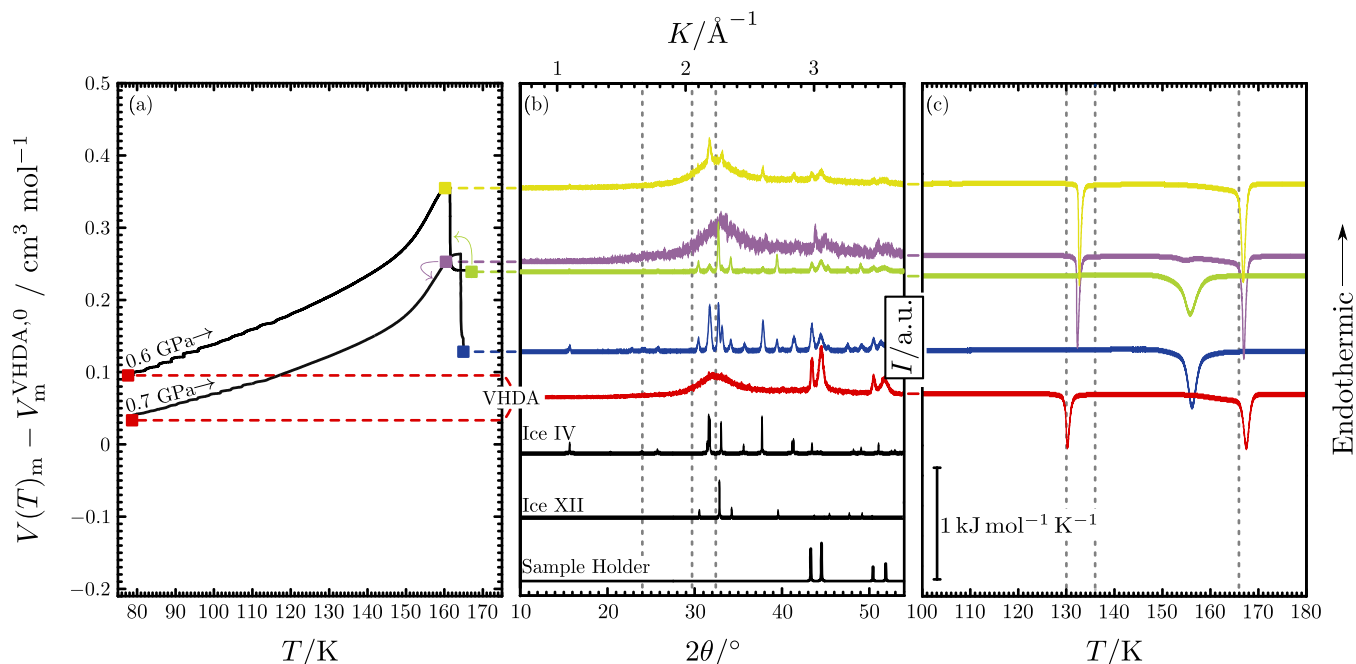


FIG. 5. Analogous to Fig. 3 for heating of VHDA at 0.6 and 0.7 GPa. The green point belongs to the experiment at 0.6 GPa and the purple to the experiment at 0.7 GPa as indicated by the arrows. The black diffractograms at the bottom of (b) are calculated diffractograms of ice IV, ice XII and the sample holder.

Having set the stage for a proper understanding of the XRD and DSC data, we now turn to the interpretation. The XRD measurements corresponding to samples quenched before the sharp volume step show a fully amorphous diffraction pattern [see part (b) of Figs. 3–5], where the halo peak shifts to lower angles upon heating. This shift is summarized for the whole pressure range (0.10–0.70 GPa) in Fig. 6(a). At 0.10 GPa, the shift amounts to  $3.0^\circ$  and decreases to  $0.5^\circ$  at 0.5 GPa. At 0.6 and 0.7 GPa, practically no shift occurs prior to crystallization. This is consistent with the volume changes in Fig. 2(a): at 0.10 GPa, a volume change of  $2.8 \text{ cm}^3 \text{ mol}^{-1}$  takes place prior to crystallization, which shrinks to  $0.4 \text{ cm}^3 \text{ mol}^{-1}$  at 0.50 GPa. For 0.70 GPa, no more than  $0.1 \text{ cm}^3 \text{ mol}^{-1}$  expansion takes place.

Also, the results from our DSC scans agree with these findings. The samples quenched before crystallization show two exothermic peaks indicative of the amorphous nature of the samples. We summarize all corresponding onset temperatures  $T_e$  in Fig. 6(b). For 0.10 GPa,  $T_e$  shifts by 5 K, whereas for 0.50–0.70 GPa a shift of 2 K is observed. As we showed in a previous study, such a shift indicates relaxation.<sup>20</sup> Again, the samples heated at low pressures show a significant amount of relaxation, whereas barely any relaxation is visible at higher pressures.

The dashed lines in Figs. 6(a) and 6(b) indicate reference measurements for VHDA, eHDA, and LDA. Clearly, VHDA progresses toward the eHDA reference state upon heating. At 0.1 GPa, the eHDA reference state is reached when VHDA is heated to  $\approx 140 \text{ K}$ , as judged both from XRD [Fig. 6(a)] and DSC [Fig. 6(b)]. This indicates that VHDA samples that have been decompressed at 140 K to 0.1 GPa and VHDA samples that have been decompressed at 77 K to 0.1 GPa and then heated to 140 K are at the same state. Hence, this is a case of path independence, which is a sign for equilibration in the amorphous state. This corroborates our earlier results on the nature of the transition to LDA at 4 MPa.<sup>12</sup>

The relaxation is also noted from the peak area of the first exotherm in Fig. 3(c), which reflects the heat associated with the polyamorphic transition. In VHDA itself, we here find a heat of  $-637 \text{ J mol}^{-1}$ , in agreement with the value  $-640 \pm 10 \text{ J mol}^{-1}$  reported by Winkel.<sup>33</sup> This reduces to  $-462 \pm 41 \text{ J mol}^{-1}$  after heating at 0.1 GPa. That is, the enthalpy associated with relaxation amounts to  $\approx 175 \text{ J mol}^{-1}$ .

To judge whether path-independence occurs also at other pressures studied here, we also compare our isobaric experiments with the isothermal results of Winkel *et al.*<sup>17,21</sup> in Figs. 6(c) and 6(d). Winkel *et al.* used *ex situ* XRD and

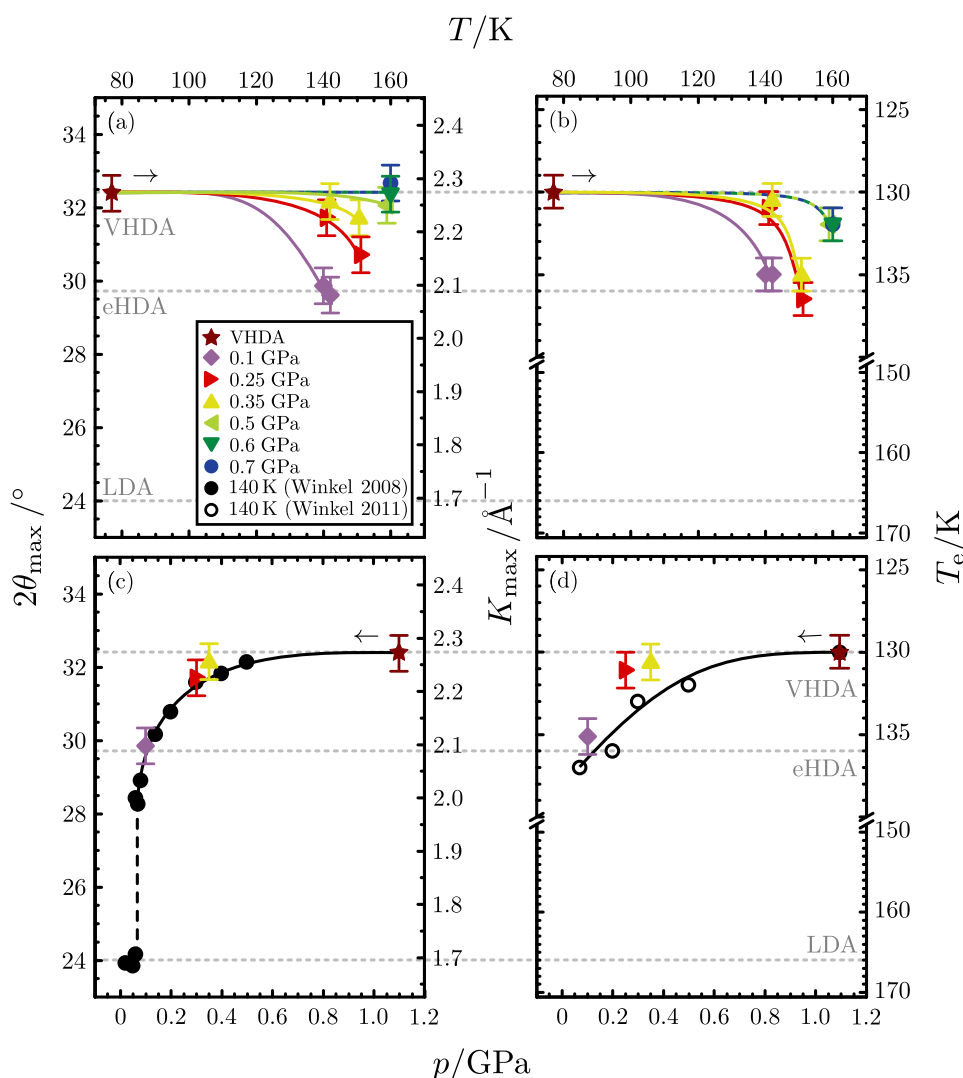


FIG. 6. Summary of the *ex situ* XRD and DSC results after the isobaric heating of VHDA. Part (a) shows the average positions of the first diffraction maximum as found in XRD as a function of the respective maximum  $T$  in the isobaric heating step. Part (b) shows the average DSC transition temperature  $T_e$  of the high-density amorphous ice as a function of the respective maximum  $T$  in the isobaric heating step. The dotted grey lines mark the values of the VHDA and eHDA reference samples, as well as the values for LDA. Solid lines are guide to the eye. Parts (c) and (d) show only data points after heating VHDA to  $\approx 140 \text{ K}$  as a function of pressure. Here also values obtained from isothermal decompression of VHDA at 140 K from Refs. 17 and 21 are shown for comparison. Please note we corrected the data of Ref. 21 to match the onset temperatures of LDA crystallization (see the supplementary material).

DSC to study the states that occur during decompression of VHDA at 140 K. Hence, if our results for samples heated to 140 K coincide with the data points from Refs. 17 and 21, path independence is confirmed. First, we note that the data point after heating VHDA at 0.1 GPa to 140 K coincides with Winkel *et al.*'s data, confirming the above found path independence. After heating at 0.25 GPa to 141 K, the XRD data point comes very close to Winkel *et al.*'s [cf. Fig. 6(c)] suggesting path-independence, whereas the DSC point does not [cf. Fig. 6(d)]. For all higher pressures, heating to significantly higher temperatures was necessary to match Winkel *et al.*'s data both in XRD and DSC. Thus, path-independence is not the case at  $p > 0.25$  GPa. Hence, metastable equilibrium is definitely reached at 140 K and 0.1 GPa, it is close at 140 K and 0.25 GPa, and it is not reached at higher pressures, consistent with previous results.<sup>12,21</sup>

That is, the isobaric heating of VHDA at  $0.1 \leq p \leq 0.7$  GPa results in a continuous relaxation followed by crystallization. The characterizations employed indicate that the relaxation yields states varying continuously from VHDA at high pressures to eHDA at low pressures, consistent with similar isothermal experiments<sup>17,18</sup> as well as isobaric experiments at 1 bar<sup>13,14,16</sup> and 4 MPa.<sup>12</sup> The crystallization behavior will be discussed in Sec. V.

#### IV. ISOBARIC HEATING OF eHDA

##### A. Analysis of the volume curves

The volume curves of the isobaric heating experiments of eHDA in the metastability domain of VHDA are shown

in Fig. 2(b). The reference for these volume curves is an eHDA sample at 0.1 GPa. The starting points of the curves reflect the volume change incurred upon compressing eHDA at 77 K, i.e., the curves show  $V_m(T) - V_m^{\text{eHDA}}(77 \text{ K}, 0.1 \text{ GPa})$ . All curves show that the samples densify during heating. This densification progresses in a continuous fashion, indicating that only a relaxation takes place. We stopped the heating prior to the crystallization temperature  $T_X$ , and so no sharp steps are seen [by contrast to Fig. 2(a)]. A notable exception occurred in one experiment at 1.3 GPa, where a sharp step upon reaching 160 K was observed, marking the crystallization of the sample. This experiment is discussed in the [supplementary material](#).

##### B. XRD and DSC analysis

For the eHDA experiments, no samples were quenched in the smooth densification step. Therefore, all characterizations performed yield only information about the state reached after heating to 160 K. Figure 7 is designed in analogy to Figs. 3–5. The volume curves from Fig. 2(b) are reproduced (left panel), and the XRD scans (middle panel) and the DSC scans (right panel) are shown in the same colour code and are connected by dashed horizontal lines.

Both the XRD and DSC measurements show that all samples are mainly amorphous after the heating procedure, although crystalline traces were found. Figures 8(a) and 8(b) summarize the position of the first halo peak  $2\theta_{\text{max}}$  and the polyamorphic transition temperature  $T_e$ , respectively. Just like in the VHDA case, the heating step produces a shift both in the position of the first diffraction maximum and in  $T_e$ . After

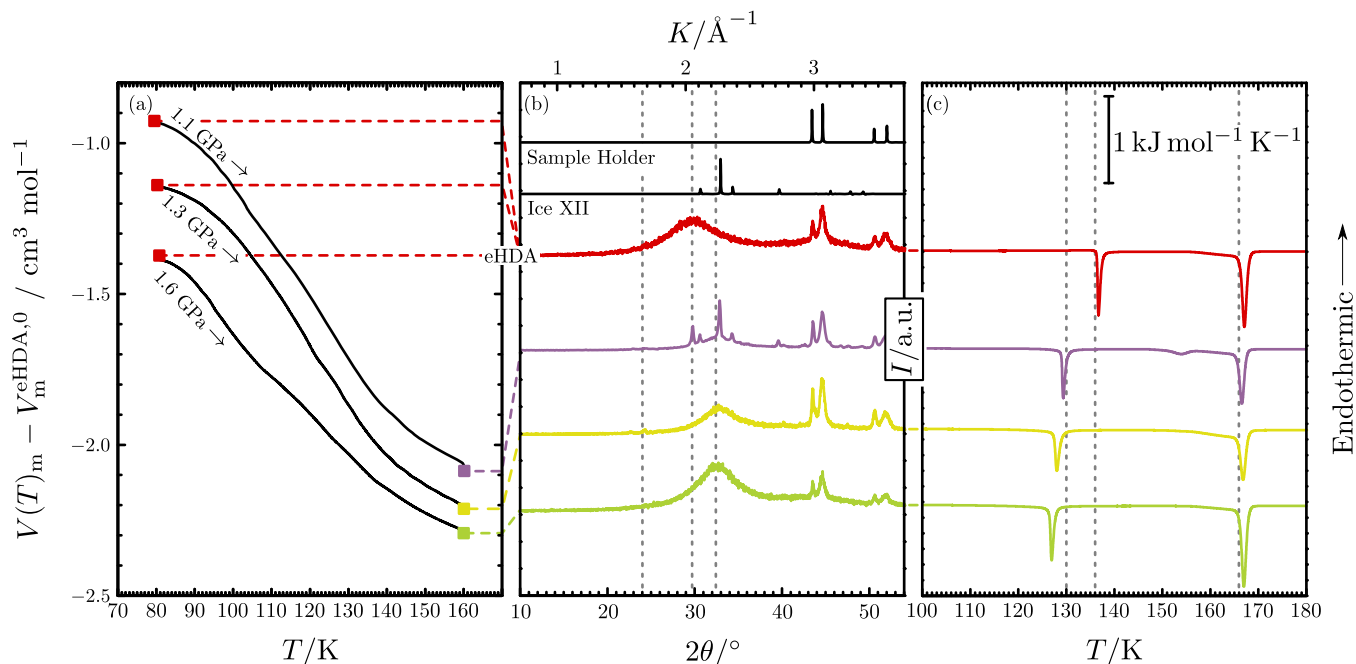


FIG. 7. XRD and DSC-analysis of initial and final states of the isobaric heating of eHDA at high pressures. (a) shows the volume change of the complete transition. The corresponding diffractograms and calorigrams after quench-recovery are shown in (b) and (c), respectively. In (b), the dotted grey line at  $24.0^\circ$  ( $1.69 \text{ \AA}^{-1}$ ) marks the position of the first diffraction maximum for LDA according to Refs. 80 and 32. The dotted grey lines at  $29.7^\circ$  ( $2.09 \text{ \AA}^{-1}$ ) and at  $32.4^\circ$  ( $2.26 \text{ \AA}^{-1}$ ) mark the position of the first diffraction maximum of the eHDA and VHDA references, respectively. The black diffractograms at the bottom of (b) are calculated diffractograms of ice XII and the sample holder. In (c), the dotted grey lines at 130, 136, and 166 K mark the onset temperature of the VHDA  $\rightarrow$  LDA, eHDA  $\rightarrow$  LDA, and LDA  $\rightarrow$  I<sub>c</sub> transition, respectively.

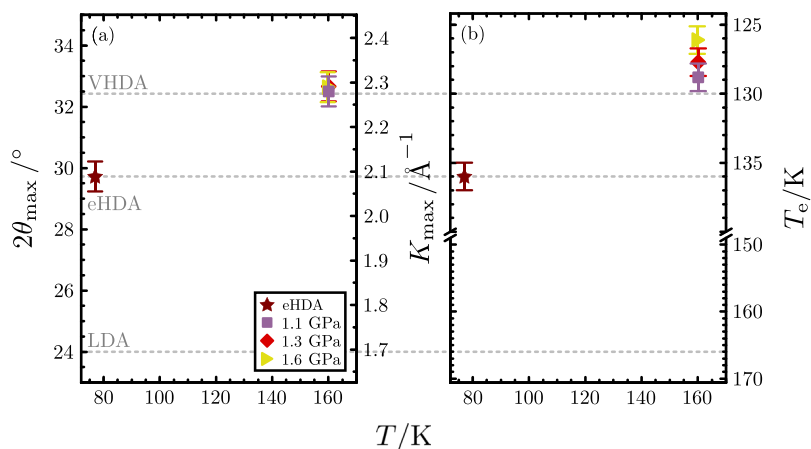


FIG. 8. Summary of the *ex situ* XRD and DSC results after the isobaric heating of eHDA to 160 K. Part (a) shows the average positions of the first diffraction maximum as found in XRD after heating and part (b) shows the average DSC transition temperature  $T_e$  of the high-density amorphous after heating. At each pressure, three different samples were studied. The dotted grey lines mark the values of the VHDA and eHDA reference samples, as well as the values for LDA.

heating to 160 K, the halo maximum reaches the VHDA reference [dashed line in Fig. 8(a)]. In addition,  $T_e$  shifts to lower temperatures. It reaches 129, 128, and 126 K for 1.1, 1.3, and 1.6 GPa, respectively [cf. Fig. 8(b)]. That is, with increasing pressure, there is a slight deviation from the VHDA reference that was prepared at 1.1 GPa.

The heat of the polyamorphic transition recorded in DSC after the isobaric heating is  $-703 \pm 47 \text{ J mol}^{-1}$  for 1.3 GPa and  $-719 \pm 56 \text{ J mol}^{-1}$  for 1.6 GPa. These values are slightly higher as the one found for our VHDA reference sample ( $-637 \text{ J mol}^{-1}$ ) and the value reported by Winkel<sup>33</sup> ( $-640 \pm 10 \text{ J mol}^{-1}$ ), both of which were prepared at 1.1 GPa. This indicates that at higher pressure denser VHDA forms, which shows higher transition enthalpies to LDA.

That is, isobaric heating of eHDA at  $1.1 \leq p \leq 1.6 \text{ GPa}$  to 160 K leads to a continuous densification in all cases. As apparent from the XRD and DSC characterizations, the heating produces states that are VHDA or close to it.

## V. CRYSTALLIZATION EVENTS

### A. VHDA

As discussed in Sec. III, the heating of VHDA at  $0.1 \leq p \leq 0.7 \text{ GPa}$  always terminates in a sharp volume step indicating the crystallization of the sample. If we take the temperature of the volume step as the crystallization temperature of VHDA, we find that VHDA crystallizes at significantly higher temperatures than uHDA. This becomes obvious in Fig. 9, where all the crystallization temperatures obtained from the volume curves in Fig. 2(a) (red triangles connected by a solid line) are compared with literature data (all other symbols).<sup>29,30,68,75-77</sup> The assignment of the sharp step to a crystallization event is corroborated from our XRD and DSC data. After the sharp step at 0.10 GPa [Fig. 3(a)], the XRD scan shows sharp Bragg peaks [Fig. 3(b)] and the DSC scan shows only a single exotherm [Fig. 3(c)]. In the [supplementary material](#), we show the phase composition after crystallization, which is consistent with the idea that both eHDA<sup>75,76</sup> and VHDA<sup>77</sup> differ from uHDA in that in the latter nanocrystalline remnants are present.

### B. eHDA

Only one out of nine samples shows a volume step before 160 K, but still XRD measurements show traces of ice XII. At 1.1 GPa, no measurement out of six performed (two per sample) was free of crystalline reflexes, and at 1.3 GPa only one out of six and at 1.6 GPa five out of seven contained no crystalline reflexes. The sheer occurrence of crystalline traces at 160 K is surprising, when considering the known crystallization temperatures at these pressures (cf. Fig. 9). This finding may be explained by the very recent study of Tonauer *et al.*,<sup>78</sup> who demonstrated the presence of nanocrystalline domains in eHDA produced by decompression to 0.1 GPa. According to this work, nanocrystalline domains form upon compression from LDA-nanodomains, which themselves appear in the eHDA preparation step at  $\leq 0.10 \text{ GPa}$  at 140 K. Since our eHDA samples were prepared that way, they presumably contain

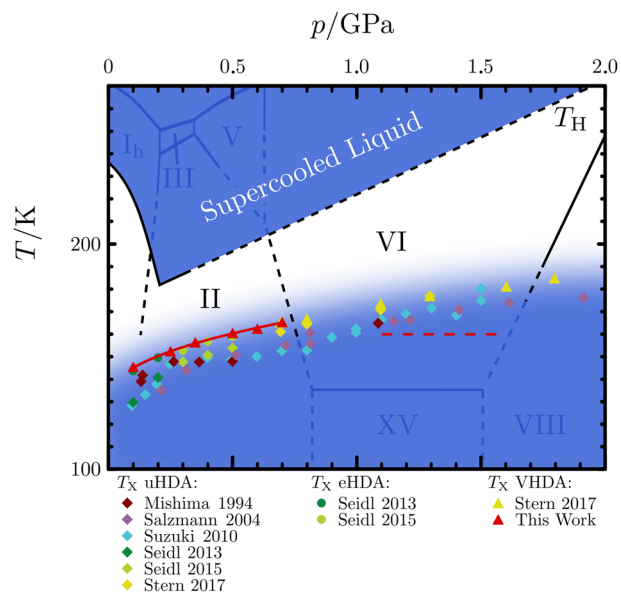


FIG. 9. Phase diagram of water based on Refs. 1, 58, 81, and 82 highlighting the liquid and high-density amorphous phase. For HDA and VHDA, the crystallization temperatures found in this work are compared with data from the literature.<sup>29,30,68,75-77</sup> The dashed red line indicates the temperature where we find crystalline traces after heating eHDA.

crystalline traces that continuously grow from nanocrystalline domains.<sup>78</sup>

## VI. SUMMARY AND CONCLUSION

We studied the behavior of VHDA and eHDA by *in situ* volumetry upon isobaric heating at  $0.1 \leq p \leq 0.7$  GPa and  $1.1 \leq p \leq 1.6$  GPa, respectively, in search of sharp limits of stability. No such sharp limit was observed in any of the experiments reported here, but instead a continuous relaxation process followed by a sharp crystallization. For VHDA a pronounced volume relaxation takes place at lower pressures, which proceeds through a continuum of states in between VHDA and eHDA. In addition, the transformation from eHDA to VHDA at high pressures appears as a continuous densification, and all isobaric transformations studied here are clearly less sharp than the isobaric eHDA  $\rightarrow$  LDA transition.<sup>12,20,21</sup> The continuous nature of the isobaric VHDA  $\rightarrow$  eHDA and eHDA  $\rightarrow$  VHDA transitions is consistent with several other results.<sup>12–14,16–18,28–30,33–36</sup> This suggests that there is a continuum of states between VHDA and HDA at least in the temperature range studied here, i.e., at  $T \geq 77$  K. At such temperatures, eHDA and VHDA can be regarded as two extreme cases of HDA. VHDA being the most relaxed amorphous ice at high pressures, in accordance with its apparent similarity to HDL,<sup>26,34,47,49</sup> and eHDA being the most relaxed HDA at low pressures, as apparent from its high thermal stability at ambient pressure.<sup>19–21</sup> Nevertheless, the possible maximum in  $T_g$ <sup>23,24</sup> and the second density jump upon isothermal compression of LDA at 125 K<sup>25</sup> still demand an explanation. We suggest that sufficiently slow isothermal experiments in the pressure range of interest ( $\approx 0.8$  GPa) might reveal a first-order-like transition between HDA and VHDA, similar to the experiment reported previously at 125 K.<sup>25</sup> Future work will be required to check this suggestion and to verify or falsify the existence of the binodal shown in Fig. 1(a).

Irrespective of the answer to this question, the practical importance of VHDA is without a doubt. Several recent studies show that uHDA produced along Mishima's path<sup>8</sup> is most likely not a fully amorphous material.<sup>13,14,29,75–77,79</sup> If however uHDA is annealed at high pressure, VHDA is obtained<sup>10</sup> and VHDA is most likely fully amorphous.<sup>13,14,29,77,79</sup> If this fully amorphous VHDA is subsequently decompressed at 140 K to obtain eHDA,<sup>17</sup> the fully amorphous nature is inherited by eHDA.<sup>75,76</sup> Besides the fully amorphous nature, VHDA (and eHDA at low  $p$ ) show a higher crystallization temperature than uHDA (cf. Fig. 9), extending the field of possible experiments in unknown parts of the no-man's land, possibly into regions where the amorphous ice turns into an ultraviscous liquid.<sup>6</sup> Hence, we conclude that VHDA is the proper amorphous ice to be studied at pressures above 0.8 GPa.

## SUPPLEMENTARY MATERIAL

See [supplementary material](#) for a more detailed discussion of the crystallization events observed in this study as well as for a brief discussion on DSC onset temperatures.

## ACKNOWLEDGMENTS

We thank Katrin Amann-Winkel for helpful discussions. P.H.H. and T.L. gratefully acknowledge funding by the Austrian Science Fund FWF (Erwin Schrödinger Fellowship No. J3811 N34 and bilateral Project No. I1392, respectively).

- <sup>1</sup>M. Chaplin, <http://www.lsbu.ac.uk/water/>, 2017.
- <sup>2</sup>C. A. Angell, *Annu. Rev. Phys. Chem.* **55**, 559–583 (2004).
- <sup>3</sup>P. G. Debenedetti, *J. Phys.: Condens. Matter* **15**(45), R1669–R1726 (2003).
- <sup>4</sup>P. Gallo, K. Amann-Winkel, C. A. Angell, M. A. Anisimov, F. Caupin, C. Chakravarty, E. Lascaris, T. Loerting, A. Z. Panagiotopoulos, J. Russo *et al.*, *Chem. Rev.* **116**(13), 7463–7500 (2016).
- <sup>5</sup>P. H. Poole, F. Sciortino, U. Essmann, and H. Stanley, *Nature* **360**(6402), 324–328 (1992).
- <sup>6</sup>P. H. Handle, T. Loerting, and F. Sciortino, *Proc. Natl. Acad. Sci. U. S. A.* **114**(51), 13336–13344 (2017).
- <sup>7</sup>O. Mishima and H. Stanley, *Nature* **396**(6709), 329–335 (1998).
- <sup>8</sup>O. Mishima, L. D. Calvert, and E. Whalley, *Nature* **310**(5976), 393–395 (1984).
- <sup>9</sup>O. Mishima, L. D. Calvert, and E. Whalley, *Nature* **314**(6006), 76–78 (1985).
- <sup>10</sup>T. Loerting, C. Salzmann, I. Kohl, E. Mayer, and A. Hallbrucker, *Phys. Chem. Chem. Phys.* **3**(24), 5355–5357 (2001).
- <sup>11</sup>T. Loerting, C. G. Salzmann, K. Winkel, and E. Mayer, *Phys. Chem. Chem. Phys.* **8**(24), 2810–2818 (2006).
- <sup>12</sup>P. H. Handle and T. Loerting, *J. Chem. Phys.* **148**(12), 124508 (2018).
- <sup>13</sup>M. Koza, T. Hansen, R. P. May, and H. Schober, *J. Non-Cryst. Solids* **352**(42–49), 4988–4993 (2006).
- <sup>14</sup>M. M. Koza, B. Geil, K. Winkel, C. Köhler, F. Czeschka, M. Scheuermann, H. Schober, and T. Hansen, *Phys. Rev. Lett.* **94**(12), 125506 (2005).
- <sup>15</sup>T. Loerting, K. Winkel, M. Seidl, M. Bauer, C. Mitterdorfer, P. H. Handle, C. G. Salzmann, E. Mayer, J. L. Finney, and D. T. Bowron, *Phys. Chem. Chem. Phys.* **13**(19), 8783–8794 (2011).
- <sup>16</sup>M. Scheuermann, B. Geil, K. Winkel, and F. Fujara, *J. Chem. Phys.* **124**(22), 224503 (2006).
- <sup>17</sup>K. Winkel, M. S. Elsaesser, E. Mayer, and T. Loerting, *J. Chem. Phys.* **128**(4), 044510 (2008).
- <sup>18</sup>K. Winkel, M. Bauer, E. Mayer, M. Seidl, M. S. Elsaesser, and T. Loerting, *J. Phys.: Condens. Matter* **20**(49), 494212 (2008).
- <sup>19</sup>R. J. Nelmes, J. S. Loveday, T. Strässle, C. L. Bull, M. Guthrie, G. Hamel, and S. Klotz, *Nat. Phys.* **2**(6), 414–418 (2006).
- <sup>20</sup>P. H. Handle, M. Seidl, and T. Loerting, *Phys. Rev. Lett.* **108**(22), 225901 (2012).
- <sup>21</sup>K. Winkel, E. Mayer, and T. Loerting, *J. Phys. Chem. B* **115**(48), 14141–14148 (2011).
- <sup>22</sup>C. G. Salzmann, T. Loerting, S. Klotz, P. W. Mirwald, A. Hallbrucker, and E. Mayer, *Phys. Chem. Chem. Phys.* **8**(3), 386–397 (2006).
- <sup>23</sup>P. H. Handle and T. Loerting, *Phys. Rev. B* **93**(6), 064204 (2016).
- <sup>24</sup>T. Loerting, V. Fuentes-Landete, P. H. Handle, M. Seidl, K. Amann-Winkel, C. Gainaru, and R. Böhmer, *J. Non-Cryst. Solids* **407**, 423–430 (2015).
- <sup>25</sup>T. Loerting, W. Schustereder, K. Winkel, C. G. Salzmann, I. Kohl, and E. Mayer, *Phys. Rev. Lett.* **96**(2), 025702 (2006).
- <sup>26</sup>J. L. Finney, D. T. Bowron, A. K. Soper, T. Loerting, E. Mayer, and A. Hallbrucker, *Phys. Rev. Lett.* **89**(20), 205503 (2002).
- <sup>27</sup>J. L. Finney, A. Hallbrucker, I. Kohl, A. K. Soper, and D. T. Bowron, *Phys. Rev. Lett.* **88**(22), 225503 (2002).
- <sup>28</sup>O. Mishima, *Nature* **384**(6609), 546–549 (1996).
- <sup>29</sup>Y. Suzuki and Y. Tominaga, *J. Chem. Phys.* **133**(16), 164508 (2010).
- <sup>30</sup>O. Mishima, *J. Chem. Phys.* **100**(8), 5910–5912 (1994).
- <sup>31</sup>Y. Yoshimura, H. Mao, and R. J. Hemley, *Chem. Phys. Lett.* **420**(4–6), 503–506 (2006).
- <sup>32</sup>K. Winkel, D. Bowron, T. Loerting, E. Mayer, and J. L. Finney, *J. Chem. Phys.* **130**(20), 204502 (2009).
- <sup>33</sup>K. Winkel, “Study of amorphous-amorphous transitions in water,” Ph.D. thesis, Verlag Dr. Hut GmbH, 2009.
- <sup>34</sup>S. Klotz, G. Hamel, J. S. Loveday, R. J. Nelmes, M. Guthrie, and A. K. Soper, *Phys. Rev. Lett.* **89**(28), 285502 (2002).
- <sup>35</sup>S. Klotz, T. Strässle, A. M. Saitta, G. Rousse, G. Hamel, R. J. Nelmes, J. S. Loveday, and M. Guthrie, *J. Phys.: Condens. Matter* **17**(11), S967–S974 (2005).
- <sup>36</sup>Y. Suzuki and O. Mishima, *J. Phys.: Condens. Matter* **21**(15), 155105 (2009).

- <sup>37</sup>A.-A. Ludl, L. Bove, A. Saitta, M. Salanne, T. Hansen, C. Bull, R. Gaal, and S. Klotz, *Phys. Chem. Chem. Phys.* **17**(21), 14054–14063 (2015).
- <sup>38</sup>L. E. Bove, S. Klotz, J. Philippe, and A. M. Saitta, *Phys. Rev. Lett.* **106**(12), 125701 (2011).
- <sup>39</sup>S. V. Buldyrev and H. Stanley, *Phys. A* **330**(1-2), 124–129 (2003).
- <sup>40</sup>P. Jedlovsky and R. Vallauri, *J. Chem. Phys.* **122**(8), 081101 (2005).
- <sup>41</sup>D. Paschek, A. Rüppert, and A. Geiger, *ChemPhysChem* **9**(18), 2737–2741 (2008).
- <sup>42</sup>I. Brovchenko, A. Geiger, and A. Oleinikova, *J. Chem. Phys.* **118**(21), 9473–9476 (2003).
- <sup>43</sup>I. Brovchenko, A. Geiger, and A. Oleinikova, *J. Chem. Phys.* **123**(4), 044515 (2005).
- <sup>44</sup>N. Giovambattista, P. G. Debenedetti, F. Sciortino, and H. E. Stanley, *Phys. Rev. E* **71**(6), 061505 (2005).
- <sup>45</sup>N. Giovambattista, H. E. Stanley, and F. Sciortino, *Phys. Rev. E* **72**(3), 031510 (2005).
- <sup>46</sup>R. Martonák, D. Donadio, and M. Parrinello, *Phys. Rev. Lett.* **92**(22), 225702 (2004).
- <sup>47</sup>B. Guillot and Y. Guissani, *J. Chem. Phys.* **119**(22), 11740–11752 (2003).
- <sup>48</sup>R. Martonák, D. Donadio, and M. Parrinello, *J. Chem. Phys.* **122**(13), 134501 (2005).
- <sup>49</sup>N. Giovambattista, H. E. Stanley, and F. Sciortino, *Phys. Rev. Lett.* **94**(10), 107803 (2005).
- <sup>50</sup>Y. Liu, A. Z. Panagiotopoulos, and P. G. Debenedetti, *J. Chem. Phys.* **131**(10), 104508 (2009).
- <sup>51</sup>S. Klotz, T. Strässle, R. J. Nelmes, J. S. Loveday, G. Hamel, G. Rousse, B. Canny, J. C. Chervin, and A. M. Saitta, *Phys. Rev. Lett.* **94**(2), 025506 (2005).
- <sup>52</sup>M. S. Elsaesser, I. Kohl, E. Mayer, and T. Loerting, *J. Phys. Chem. B* **111**(28), 8038–8044 (2007).
- <sup>53</sup>K. Winkel, W. Schustereder, I. Kohl, C. G. Salzmann, E. Mayer, and T. Loerting, in *Physics and Chemistry of Ice*, Special Publications, edited by W. Kuhs (The Royal Society of Chemistry, 2007), pp. 641–648.
- <sup>54</sup>H. Engelhardt and B. Kamb, *J. Glaciol.* **21**(85), 51–53 (1978).
- <sup>55</sup>W. F. Kuhs, D. V. Bliss, and J. L. Finney, *J. Phys. Colloq.* **48**(C1), C1-631–C1-636 (1987).
- <sup>56</sup>W. F. Kuhs and M. S. Lehmann, in *Water Science Reviews 2: Volume 2, Crystalline Hydrates*, edited by F. Franks (Cambridge University Press, 1986), pp. 1–65.
- <sup>57</sup>V. F. Petrenko and R. W. Whitworth, *Physics of Ice* (Oxford University Press, 1999).
- <sup>58</sup>C. Lobban, J. L. Finney, and W. F. Kuhs, *Nature* **391**(6664), 268–270 (1998).
- <sup>59</sup>M. Koza, H. Schober, A. Tölle, F. Fujara, and T. Hansen, *Nature* **397**(6721), 660–661 (1999).
- <sup>60</sup>C. Lobban, J. L. Finney, and W. F. Kuhs, *J. Chem. Phys.* **112**(16), 7169–7180 (2000).
- <sup>61</sup>H. Engelhardt and B. Kamb, *J. Chem. Phys.* **75**(12), 5887–5899 (1981).
- <sup>62</sup>L. G. Dowell and A. P. Rinfret, *Nature* **188**(4757), 1144–1148 (1960).
- <sup>63</sup>K. Röttger, A. Endriss, J. Ihringer, S. Doyle, and W. F. Kuhs, *Acta Crystallogr., Sect. B: Struct. Sci.* **50**(6), 644–648 (1994).
- <sup>64</sup>H. E. Swanson and E. Tatge, *Standard X-Ray Diffraction Powder Patterns, Volume I of National Bureau of Standards Circular* (U.S. Department of Commerce, National Bureau of Standards, 1953).
- <sup>65</sup>P. H. Handle, “Relaxationsdynamik in hochdichtem amorphem Eis,” M.Sc. thesis, Universität Innsbruck, 2010.
- <sup>66</sup>Y. Handa, O. Mishima, and E. Whalley, *J. Chem. Phys.* **84**(5), 2766–2770 (1986).
- <sup>67</sup>M. A. Floriano, Y. P. Handa, D. D. Klug, and E. Whalley, *J. Chem. Phys.* **91**(11), 7187–7192 (1989).
- <sup>68</sup>C. G. Salzmann, E. Mayer, and A. Hallbrucker, *Phys. Chem. Chem. Phys.* **6**(6), 1269–1276 (2004).
- <sup>69</sup>J. E. Bertie, L. D. Calvert, and E. Whalley, *J. Chem. Phys.* **38**(4), 840–846 (1963).
- <sup>70</sup>Y. Handa, D. D. Klug, and E. Whalley, *Can. J. Chem.* **66**(4), 919–924 (1988).
- <sup>71</sup>I. Kohl, E. Mayer, and A. Hallbrucker, *J. Phys. Chem. B* **104**(51), 12102–12104 (2000).
- <sup>72</sup>C. G. Salzmann, I. Kohl, T. Loerting, E. Mayer, and A. Hallbrucker, *Phys. Chem. Chem. Phys.* **5**(16), 3507 (2003).
- <sup>73</sup>W. F. Kuhs, C. Sippel, A. Falenty, and T. C. Hansen, *Proc. Natl. Acad. Sci. U. S. A.* **109**(52), 21259–21264 (2012).
- <sup>74</sup>T. L. Malkin, B. J. Murray, C. G. Salzmann, V. Molinero, S. J. Pickering, and T. F. Whale, *Phys. Chem. Chem. Phys.* **17**(1), 60–76 (2015).
- <sup>75</sup>M. Seidl, K. Amann-Winkel, P. H. Handle, G. Zifferer, and T. Loerting, *Phys. Rev. B* **88**(17), 174105 (2013).
- <sup>76</sup>M. Seidl, A. Fayter, J. N. Stern, G. Zifferer, and T. Loerting, *Phys. Rev. B* **91**(14), 144201 (2015).
- <sup>77</sup>J. Stern and T. Loerting, *Sci. Rep.* **7**, 3995 (2017).
- <sup>78</sup>C. M. Tonauer, M. Seidl-Nigsch, and T. Loerting, *J. Phys.: Condens. Matter* **30**(3), 034002 (2018).
- <sup>79</sup>M. M. Koza, R. P. May, and H. Schober, *J. Appl. Crystallogr.* **40**(s1), s517–s521 (2007).
- <sup>80</sup>A. Bizid, L. Bosio, A. Defrain, and M. Oumezzine, *J. Chem. Phys.* **87**(4), 2225–2230 (1987).
- <sup>81</sup>C. G. Salzmann, P. G. Radaelli, B. Slater, and J. L. Finney, *Phys. Chem. Chem. Phys.* **13**(41), 18468–18480 (2011).
- <sup>82</sup>H. Kanno, R. J. Speedy, and C. A. Angell, *Science* **189**(4206), 880–881 (1975).